# Three-dimensional Displacement Measurements Using Digital Image Correlation and Photogrammic Analysis

by Z.L. Kahn-Jetter and T.C. Chu

ABSTRACT—The application of digital image correlation and stereoscopic principles is used to determine three-dimensional displacements. Two pairs of stereo images of a speckled surface before and after deformation are digitized and correlated to determine the three-dimensional displacements. The images are interpolated so as to account for subpixel displacements. A sequential decision technique and a coarse-fine search are employed to increase computer efficiency and decrease run time. Very accurate results are obtained, especially when the magnification is increased. The effect of camera tilt is shown to be negligible. Theory and experimental verification are presented.

## Introduction

Recently, there has been considerable development in the application of digital image correlation and speckle patterns to determine, experimentally, strains and displacements on loaded bodies. A speckle effect, or random dot pattern, can be produced by various methods. For example, when a diffuse surface is illuminated by coherent radiation, laser speckles are achieved.[1] Similarly, acoustical speckles are produced when ultrasound irradiates a surface (or the interior of an object.)[2] Speckle patterns can also be generated by spraying paint on a surface.[3]

The theory and procedure involved in digitizing and correlating (or comparing mathematically) an image of a speckle pattern before the body is deformed with a digitized image of the speckle pattern of a deformed body is described by Chu *et al.*[4] Applications of this procedure in rigid-body mechanics, specifically to the measurement of in-plane displacements and strains, are also presented in the literature.[5-7]

The application of stereoscopic principles to digital image correlation techniques lends itself to the determination of three-dimensional displacements. Photogrammetry involves two cameras (or one camera in a moving vehicle) with the line of sight normal to the plane of the object, separated a specific amount so as to maintain an overlap of their respective views. From the geometry involved, the planar coordinates of the object relative to some fixed point can be determined. Also, the elevation relative to the average distance between the lens and the object can be determined from the stereoscopic parallax. This parallax, or the disparity between the two images, is by definition the offset of the image of the object on one camera's image-sensing plane relative to the other.

Photogrammic principles have been used extensively for more than 100 years for surveying. More recently, it has been applied to machine, or computer, vision tasks such as range sensing, parts inspection and metrology.[8] One of the key issues involved in stereo depth measurement is the identification of the same points in the two images that correspond to points on the object. This 'correspondence' problem is addressed by many authors. Klaus and Horn,[9] and Nevatia[10] present good reviews of the literature.

The objective of this paper is to describe the application of combining stereoscopic principles, digital image correlation and speckle patterns to determine, within very reasonable accuracy, three-dimensional surface displacements on loaded bodies.

## Theory

### *Photogrammetry*

Figure 1(a) shows the geometry when two cameras are parallel to each other and are focused on the same surface. From basic optics, it can be shown that with the coordinate system chosen,

$$X = e\frac{X_R + X_L}{X_R - X_L} \tag{1}$$

$$Y = 2e\frac{Y_R}{X_R - X_L} \tag{2}$$

and

$$Z = 2e\frac{d}{X_R - X_L} \tag{3}$$

*Z.L. Kahn-Jetter (SEM Member) is Assistant Professor of Mechanical Engineering, Manhattan College, Mechanical Engineering Department, Manhattan College Parkway, Riverdale, NY 10471. T.C. Chu (SEM Member) is Assistant Professor of Mechanical Engineering, Polytechnic University, Department of Mechanical and Industrial Engineering, Brooklyn, NY 11202.*

*Original manuscript submitted: July 30, 1988. Final manuscript received: June 9, 1989.*

where $X$, $Y$, and $Z$ are coordinates of a point on the surface; $X_L$, $Y_L$, $X_R$, and $Y_R$ are the $X$ and $Y$ coordinates of the point on the image-sensing plane for the left and right views, respectively; $d$ is the distance between the camera lens and the image plane, and $e$ is one-half the distance between the two cameras. $(X_R - X_L)$ is known as the stereoscopic parallax and is usually represented by $P$. This can be seen in Fig. 1(b).

Figure 2 demonstrates the change in geometry when the object plane is displaced a distance $w$, normal to the original object plane. Due to this displacement there will be a different stereoscopic parallax, $P'$. Therefore, eq (3) can be rewritten as

$$Z - w = \frac{2ed}{P'} \tag{4}$$

Simultaneous displacements in the $X$ and $Y$ directions will not affect the results, and, furthermore, they too are directly related to the change in the parallax. Specifically,

$$\Delta X = e\left(\frac{X_R' + X_L'}{P'} - \frac{X_R + X_L}{P'}\right) \tag{5}$$

and

$$\Delta Y = 2e\left(\frac{Y_R'}{P'} - \frac{Y_R}{P}\right) \tag{6}$$

where $\Delta X$ and $\Delta Y$ are the displacements in the $X$ and $Y$ directions, respectively, and the primed coordinates are those related to the displaced point.

Solving for $P' - P$ from eqs (3) and (4), or $\Delta P$, which represents the change in the stereoscopic parallax yields

$$\Delta P = 2e\frac{d}{Z}\frac{w}{Z - w} \tag{7}$$

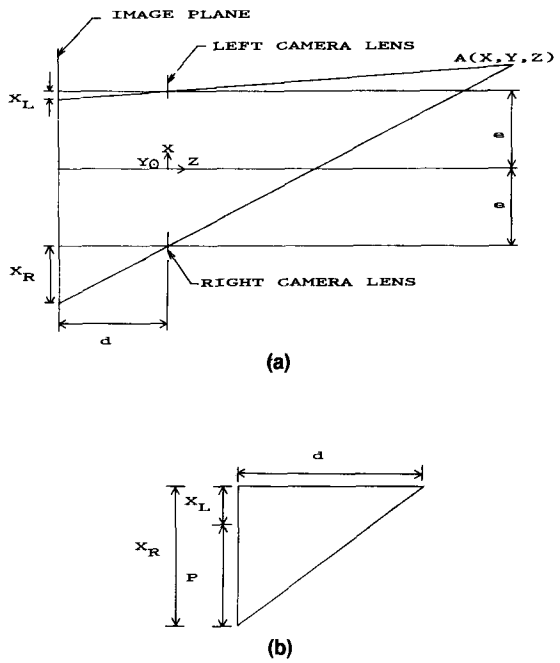


Fig. 1(a)—Stereoscopic setup, (b) stereoscopic parallax

As discussed in greater detail below, when a video image is digitized, $\Delta P$ is measured in 'pixels', or picture elements. The $\Delta P$ expressed above corresponds to a displacement on the image sensing plane, in dimensions of length. Therefore, prior to its use it must be converted to pixels in the digitized image.

One of the errors involved in photogrammic analysis is caused by camera tilt. It has previously been proven that for small angular deviations this error is small.[11] Furthermore, with the particular setup used to conduct the experiments, a tilt of five deg resulted in an error of less than $\pm 2$ percent in the calculation of $\frac{Z}{d}$.[12]

## Correlation Algorithm

It is necessary that the field of view of the two cameras encompass the point in question and that it be in focus, both before and after displacement. To identify the point in the two views, the left and right images are correlated. Denoting $u$ and $v$ as the pixel offsets from one image to the other, if $f^*(X+u, Y+v)$ represents the gray-level intensity of the speckle pattern on one image and $f(X,Y)$ represents the intensity on the other image, it is necessary to find the minimum correlation function $C(u,v)$. This function can be represented by

$$C(u,v) = \int\int |f^*(X+u, Y+v) - f(X,Y)|\,dxdy \tag{8}$$

Digital images are, of course, discrete. Therefore, the correlation function used must be converted to discrete form which can be represented by

$$C(u,v) = \sum_{\Delta M} |f^*(X+u, Y+v) - f(X,Y)| \tag{9}$$

where $\Delta M$ is a subset of the image.

This function can be normalized so as to range between 0 and 1. This is done by dividing the correlation function by the size of the subset and the maximum gray-level range. This normalized function can be expressed as

$$\overline{C}(u,v) = \frac{C(u,v)}{\Delta M(255)} \tag{10}$$

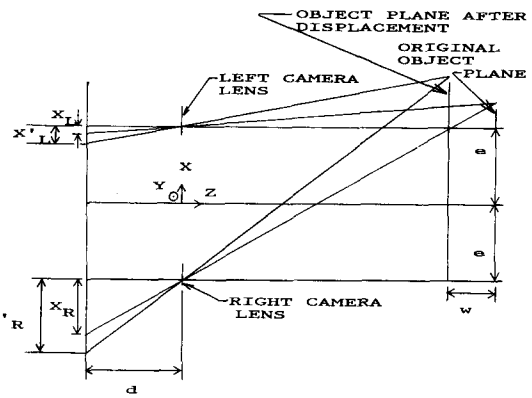


Fig. 2—Geometry due to displacement of object plane

where $\overline{C}(u,v)$ is the normalized correlation function and the gray levels for the particular system used varied between 0 and 255.

If $f(X,Y)$ represents the video or monitor image of the left image-sensing plane and $f^*(X+u, Y+v)$ represents the monitor image of the right image-sensing plane, then the determination of the minimum correlation function leads directly to the determination of the stereoscopic parallax. Thus, the coordinates of any point in space are known, relative to the coordinate system described above. To insure the same point is being studied in the images after it has been displaced, the original left image is used as a reference image and is correlated with the left and right images after displacement. This yields $(X_L', Y_L')$ and $(X_R', Y_R')$, hence, $P'$. The amount the object plane has been displaced, $w$, and the displacements in the $X$ and $Y$ directions can now be determined.

In order to increase computer efficiency and reduce run-time, two algorithms were integrated in the correlation program for this purpose. First was the use of a sequential decision technique. Wu[13] demonstrated that this reduces computer run-time significantly. A predefined threshold value is compared to the correlation function at each subset. If the correlation function exceeds this value, before the entire subset is analyzed, calculation at this subset ceases and moves on to the next subset of the image. When the correlation function is less than the threshold value at a particular subset, this correlation function then becomes the new threshold value. This procedure continues over the entire range until the minimum is found.

Second, a coarse-fine search is employed so as to account for in-between pixel matches while maintaining computer efficiency. When the minimum value of the correlation function is found at a particular integer pixel location, the image is interpolated only in this neighborhood. The sequential decision technique is employed once again for this interpolated subimage. A bilinear interpolation function was used and is described in the literature (see, for example, Refs. 3, 4 and 11).

## Experimental Apparatus and Procedure

Three types of experiments were performed to prove the validity of this technique. First was the bending of a cantilever beam. This experiment tested for monitoring out of plane displacements only on a flat surface. Second was the detection of both planar and out of plane displacements on a flat surface. Third was the stretching of an elliptical ring. This too tested for monitoring planar and out of plane displacements, however, on a curved surface. Prior to describing in detail these experiments, the hardware used and the data-acquisition procedure will be presented since the system used and the technique involved were common to all the experiments.

### *Hardware and Data Acquisition*

Figure 3 is a block diagram of the equipment used for this study. Interfaced through a multibus is an IBM PC/XT and an Imaging Technology Incorporated image processing system (ITI IP-512) consisting of four frame buffers (FB), an arithmetic logic unit (ALU), an analog processor (AP) and a histogram/feature extraction module (HF). A Javelin CCD camera with a 50-mm lens and a Hitachi monitor are also used. An entire image is stored in a frame buffer as a 512 × 512 array of 256 integer values of gray level. A 64 × 64 pixel subimage is retrieved from the frame buffer and then stored on the PC for subsequent processing.

As previously mentioned it is necessary to convert $\Delta P$ on the image-sensing plane to $\Delta P'$ on the monitor. From the optical geometry, this relationship can be expressed as

$$\Delta P' = (\Delta P)(Mo)\frac{Z}{d} \tag{11}$$

where $Mo$ is a type of magnification factor between the monitor and the object; i.e., the number of pixels of the digitized image on the monitor per unit length on the object. Substituting this into eq (7) yields

$$\Delta P' = (2e)(Mo)\frac{w}{Z-w} \tag{12}$$

It was also necessary to determine the average distance between the object plane and the lens, or, the original distance $Z$ (before object deformation). This calibration was performed by digitizing a pair of stereo images of the object plane and then displacing the camera with various known amounts away from the object while digitizing these subsequent stereo pairs of images. Correlating these images led to the determination of the changes of the stereoscopic parallax due to these known displacements. Using this as input to eq (12), a value of $Z$ could then be determined from each stereo pair. Using several displacement calibrations, an average $Z$ was calculated and used for the experiments.

### *Beam Experiment*

Ten sets of experiments were performed. The first was the deflection of a 37.66-cm × 1.27-cm × 0.96-cm cantilever aluminum beam. To test the hypothesis that out of plane deformations can be found by combining a digital image correlation algorithm with stereoscopic photogrammic analysis, the camera was placed above the beam,

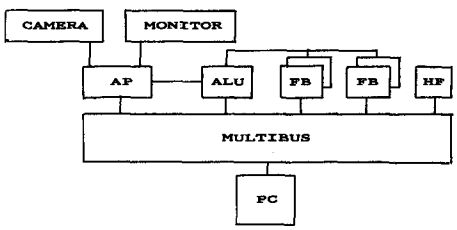

Fig. 3—Image-processing equipment

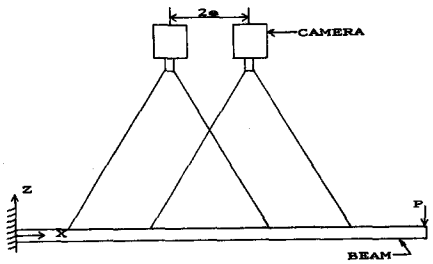

Fig. 4—Camera position with respect to beam

mounted on an $X-Y$ translation table, in the same plane as the direction of bending, as shown in Fig. 4. A photograph of the actual setup is shown in Fig. 5. A speckle pattern created by black and white spray paint was used. One point, located 28.69 cm away from the fixed end was analyzed while the deflection at the tip of the beam was increased in increments. A 15-mm extension tube was attached to the lens creating an $Mo$ of 253 pixels/cm. The lens was originally located 16.87 cm away from the plane of the beam before deflection and the 'two' cameras were separated by 1.094 cm (corresponding to a 54.1-percent overlap of their respective views). Table 1 summarizes these parameters for the ten experiments.

For the subsequent experiments, the magnification, or $Mo$, was increased to approximately 325 pixels/cm by using a 20-mm extension tube. This was done to obtain larger pixel shifts for the same deflections. $2e$ was changed to 0.7833 cm which represented a 49.8-percent overlap except in the fifth experiment where there was an approximate three-deg tilt of the camera in the $X$ direction. Therefore, the overlap for this experiment corresponded to 49.7 percent. Also, for the fourth and following experiments, the midpoint of the overlap region between the two images was used to perform the correlations. Previously, a point to the right by approximately one-fifth the distance of the overlap region was used. The sixth through tenth experiments were performed to test the consistency of the results and essentially duplicated the fourth and fifth experiments (except for the tilt).

### *Planar and Out of Plane Displacements on a Flat Surface*

This set of experiments was performed to verify the usefulness of this method in detecting both planar and out of plane displacements simultaneously. A flat metal plate with a black and white spray paint speckle pattern was clamped to an $X-Y-\theta$ translation table. The camera, still mounted on the original $X-Y$ translation table was placed in front of the object surface normal to the speckle pattern. The same camera and lens configuration as in the previous beam experiments was maintained. Figure 6 is a photograph of this setup.

Concurrent with the object being moved by various amounts in the $X$ direction, the camera was moved in varying amounts away from the object. (It was, of course, also moved in the $X$ direction to simulate the two stereo cameras.) For each combination of movements, two stereo images were digitized, stored on the PC and subsequently correlated.

### *Stretching of Elliptical Ring*

One side of a thin metal elliptical ring of thickness 0.38 mm and width 19.45 mm was clamped to a rigid fixture while the other side was clamped to a translation table. The ring was then stretched (in the $X$ direction) by moving the translation table to which it was clamped. Referring to Fig. 7, if point $c$ is the original position of the point being analyzed before the ring is pulled, after the ring is stretched it will move to $c'$. A dial indicator

TABLE 1—SUMMARY OF PARAMETERS FOR THE BEAM EXPERIMENTS

| Exp. | Length of beam, cm | Point analyzed (distance from fixed end), cm | $Mo$ pixels/cm | $Z$ (original distance between lenses and beam), cm |
|---|---|---|---|---|
| 1 | 37.66 | 28.69 | 253.0 | 16.87 |
| 2 | 30.80 | 17.18 | 325.2 | 12.96 |
| 3 | 30.80 | 27.11 | 325.2 | 12.96 |
| 4 | 30.80 | 27.27 | 325.2 | 12.96 |
| 5 | 30.80 | 26.55 | 325.0 | 13.00 |
| 6 | 30.80 | 27.58 | 323.2 | 13.59 |
| 7 | 30.80 | 27.62 | 325.0 | 12.98 |
| 8 | 30.80 | 27.38 | 324.9 | 13.41 |
| 9 | 30.80 | 27.40 | 325.5 | 13.36 |
| 10 | 30.80 | 27.42 | 325.0 | 13.79 |

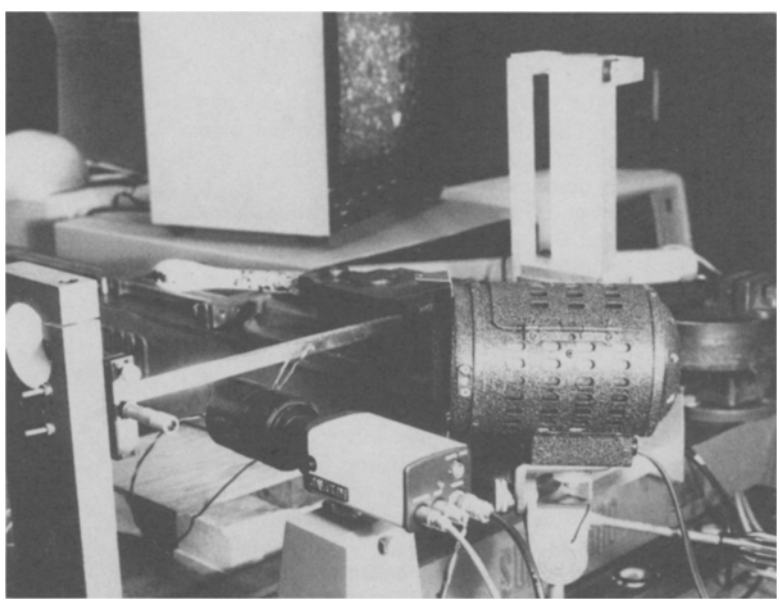

Fig. 5—Photograph of setup for beam experiment

was placed behind $c$ and measured $w_m$ (the measured displacement). However, the actual out of plane displacement was $w'$. Using the equation for an ellipse, $w'$ can be found from

$$(b - w_m) = (b - w')\sqrt{1 - (\Delta X/a')^2} \qquad (13)$$

where $b$ is the semiminor axis before stretching, $a'$ is the semimajor axis after stretching and $\Delta X$ is the amount the point traversed in the $X$ direction. By carefully monitoring $\Delta X$ and determining $w'$ from the above equation, the experimentally determined displacements were then able to be compared to the actual displacements. Figure 8 is a photograph of this experimental setup.

## Results and Discussion

### *Beam Experiment*

Figure 9 presents the results for the first five beam experiments. It is a plot of the deflections due to $\Delta P'$ versus the known deflections (calculated from the beam theory). It can be seen that in the first experiment, for which $Mo$ was equal to 253 pix/cm, the largest imposed deflections were less than 3.5 mm and, although the absolute value of the difference between the known and experimentally determined deflections were all less than 0.5 mm, errors ranged from 7.26 percent to 33.46 percent. Therefore, for the second and subsequent experiments, the magnification was increased. Although errors in the second experiment were as high as 33.14 percent (which occurred for a theoretical deflection of 0.508 mm), all the errors associated with deflections of more than 3.0 mm were less than five percent.

In the third and following experiments, the camera was moved closer to the free end of the beam so that larger deflections could be monitored (using the same setup). This greatly improved the results. As mentioned previously, in the fourth and subsequent experiments, the midpoint between the two images was used to perform the correlations. This also improved the results. For example, in the fourth experiment, the largest imposed deflection was slightly under 10 mm and the maximum error was reduced to 6.17 percent (based on a theoretical deflection of 7.787 mm). The mean absolute value of the difference between

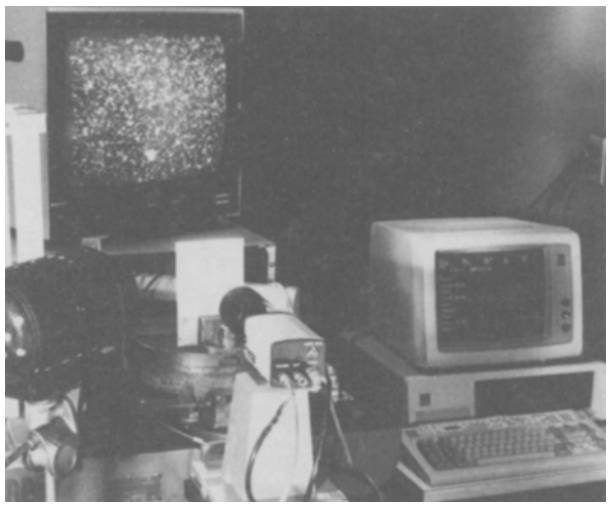

Fig. 6—Photograph of experimental setup used for analyzing planar and out of plane displacements on a flat surface

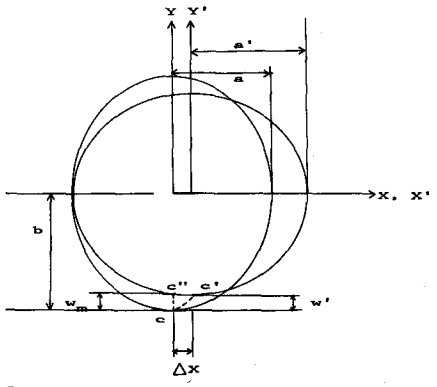


Fig. 7—Change of dimensions in stretched ring

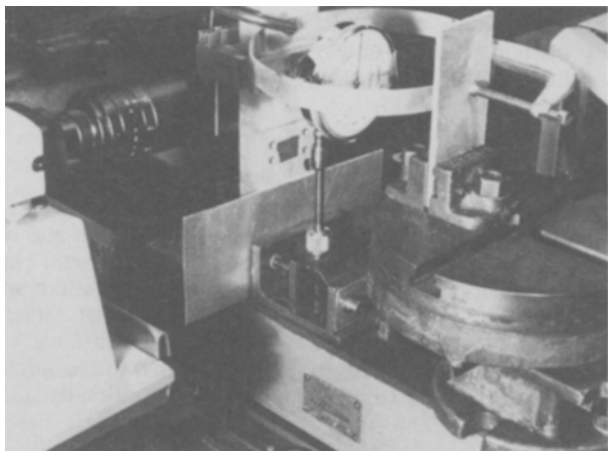

Fig. 8—Photograph of ring experiment setup

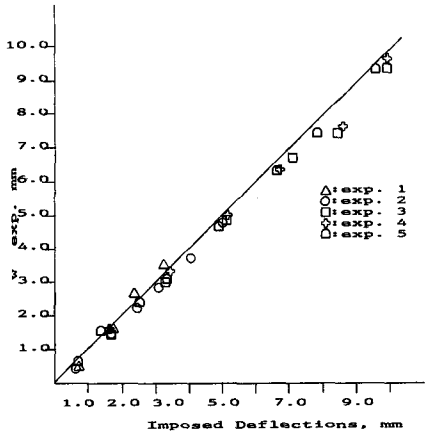


Fig. 9—A comparison of experimentally determined deflections for the first five beam experiments with imposed deflections

the theoretical and experimental deflections was 0.227 mm with a standard deviation of 0.188 mm. It is also obvious from the graph that although the camera was slightly tilted in the fifth experiment, this did not affect the results.

As mentioned earlier, the sixth through tenth experiments were performed to test the consistency of the results. Figure 10 presents the results for these experiments also as a plot of the deflections due to $\Delta P'$ versus the known deflections. In the sixth experiment, two imposed deflections were less than 1.5 mm and had errors of 39.55 percent and 33.82 percent which corresponded to a change in the stereoscopic parallax of 0.10 pixel and 1.50 pixel, respectively. Except for these two data points, it is obvious that the results are consistent.

In order to determine the actual imposed deflections, the beam equation was used. Combining the uncertainties due to measuring the beam and the fact that the micrometer which was used to bend the tip of the beam was accurate to within $\pm 0.01$ mm typically accounted for less than one-percent error.

The translation table on which the cameras was mounted (to simulate two cameras) was accurate to within $\pm 0.0025$ mm. However, interpolation of the images was either to within $\pm 0.11$ or 0.10 pixels which corresponded to a larger distance than the accuracy of the translation table.

The other errors involved were more qualitative in nature. There was slack in the movement of the $X - Y$ translation table. Besides introducing error when the camera was moved left and right (to simulate two cameras), this also introduced error when the camera was moved away from the beam to calibrate $Z$. There was also slack in the micrometer used for bending the tip of the beam. However, these 'slack problems' were negligible. There was, though, some error involved when aligning the micrometer making it just touch the tip of the beam without bending it. Actually, if this contact point for the first deflection measurement was not exact, it would, of course, cause large errors for the relatively small deflection measurements.

Probably the largest contributor of error was the noise in the image processing system. The images were digitized when there appeared to be low background noise, however, as this was done by making a visual inspection, low noise levels could not be guaranteed. For very small deflections, the change in the stereoscopic parallax, $\Delta P'$, is approximately directly proportional to the out of plane displacements [see eq (7)]. The errors associated with $\Delta P'$ of less than two pixels ranged from 1.22 percent to almost 40 percent. With the increased magnification, these pixel shifts corresponded to theoretical deflections of less than 1 mm. However, for small pixel shifts, the effect of the noise can be dramatic. Pixel shifts between approximately 3 and 18 pixels (corresponding to deflections of approximately 1.5 to 10 mm), produced significantly smaller errors (most were much less than five percent).

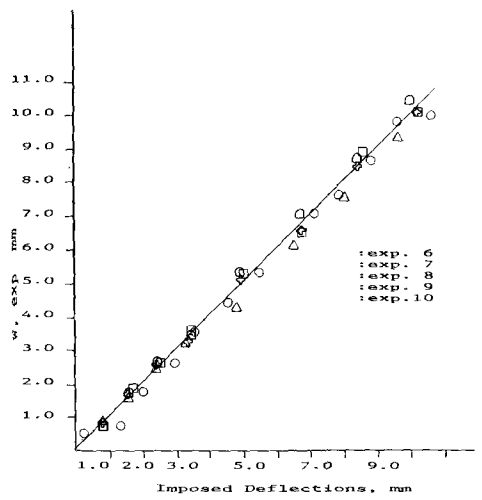


Fig. 10—A comparison of experimentally determined deflections for the last five beam experiments with imposed deflections

## Planar and Out of Plane Displacements on a Flat Surface

Table 2 presents the results for this set of experiments. It shows the mean for each experiment of $w$ actual/$w$ experimental and $\Delta X$ actual/$\Delta X$ experimental and their standard deviations. The second and third experiments were combined since $Mo$ and $Z$ were the same and there were too few data points in each experiment separately to define any meaningful statistics.

There were some errors associated with this experiment that were not involved in the beam experiments. First, there were changes in the lighting. As the plate moved in the $X$ direction, it was also moving away from the light source, causing the image to become noticeably darker. If the light had been moved, the gray-level distribution could have been changed, possibly affecting the results. Second, as larger displacements were imposed, the point being analyzed moved closer to the edges of the image. Due to the use of the extension tubes, there were distortions around the periphery of the image.

## Deformation of an Elliptical Ring

Figure 11 shows the results for this set of experiments. Three sets of experiments were performed and are represented by the different fillers in each symbol. Figure 11(a) is the measured out of plane deflections due to $\Delta P'$ versus the theoretical deflections. Figure 11(b) is the experimentally determined in-plane displacements versus the theoretical displacements. Each point in Fig. 11(a) is represented by a unique symbol so its corresponding point can be found in Fig. 11(b).

TABLE 2—RESULTS FOR PLANAR AND OUT OF PLANE DISPLACEMENTS ON A FLAT SURFACE

| Exp. | Mean $\frac{w,real}{w,\Delta P'}$ | Standard Deviation | Mean $\frac{\Delta X,real}{\Delta X,exp.}$ | Standard Deviation |
|---|---|---|---|---|
| 1 | 1.022 | 0.105 | 0.951 | 0.057 |
| 2,3 | 0.909 | 0.059 | 1.084 | 0.056 |
| 4 | 1.004 | 0.094 | 1.040 | 0.020 |
| 5 | 0.994 | 0.049 | 0.987 | 0.006 |
| 6 | 0.953 | 0.043 | 0.948 | 0.008 |
| 7 | 0.962 | 0.041 | 0.938 | 0.025 |
| 8 | 0.999 | 0.027 | 0.998 | 0.009 |
| 9 | 0.984 | 0.015 | 0.966 | 0.022 |
| 10 | 0.958 | 0.027 | 1.031 | 0.014 |
| 11 | 0.978 | 0.059 | 0.972 | 0.015 |

The same errors that were involved in the previous experiment were also involved in this one. However, since even larger planar and out of plane displacements were incurred, the lighting had to be adjusted during the course of each experiment. Also, owing to the measured accuracy of the values needed to solve for a theoretical $w'$ in eq (13), the theoretical out of plane displacement was calculated to within 0.5-percent uncertainty. Measured planar displacements were accurate to within 1.2 percent.

## Summary and Conclusions

The results can be classified into two categories. First, the results obtained on a flat surface, and, second, the results for a curved surface. Each category can also be subdivided into two groups. First, out of plane displacement measurements only, and, second, planar displacements. Most of the errors that were made on a flat surface for both planar and out of plane displacements were less than five percent. The largest error for both planar and out of plane measurements on a curved surface was less than eight percent. Most of the errors were, however, considerably smaller. For example, out of plane displacement measurements were made on a curved surface between 3.4 mm and 9.2 mm. The mean percentage error was −0.79 percent with a 4.53-percent standard deviation. Planar measurements were between 4.4 mm and 10.8 mm with a mean percentage error of −0.67 percent and a standard deviation of 2.91 percent. As mentioned earlier, the reporting of relatively large errors is somewhat misleading due to the inherent noise in the system. For example, when two images of the same speckle pattern were digitized within a short span of time (i.e., everything was kept constant and there was no movement of the object plane or the camera), theoretically, the minimum value of the correlation function should have been zero. However, that was never the case.

Three conclusions can be drawn from this study. First, the combination of stereoscopic principles, digital image correlation techniques and speckle patterns is indeed a viable method for determining three-dimensional displacements in experimental mechanics and yield reasonably accurate results. Second, the effect of camera tilt is negligible. Finally, increasing the magnification improved the results. Of course using a system with higher resolution having more gray levels and less noise will also yield more accurate results.

With the current configuration of the camera lens that was used, its range of applicability is somewhat limited. However, providing a better camera outfit including a telescopic lens, very accurate results could be obtained for much smaller deflections since larger pixel shifts would be incurred for these small displacements. Incurring larger pixel shifts would also lessen the effect of a noisy system. And, a wider selection of available lenses would be advantageous so that the use of extension tubes (which causes distortions around the periphery of the image) would not be needed. This method does have the potential of having major implications in experimental mechanics, as a nondestructive testing method. Its use is less restrictive in nature and it is not as dependent on the environment as other methods that are currently being employed. And, it has been proven that it provides a reliable means for determining the three-dimensional displacements of any point on the surface of a loaded body and can be applied to measure both in and out of plane displacements on inclined and curved surfaces.

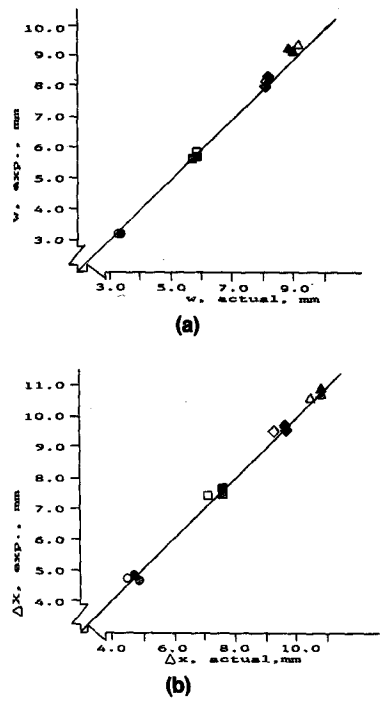


Fig. 11—A comparison of experimentally determined deflections for ring experiments with actual deflections, (a) out of plane deflections, (b) planar deflections


### Acknowledgments

The authors wish to express their appreciation to the International Business Machines Corporation for their Manufacturing Research Fellowship and equipments which were used for this study under Contract No. 486014.


### References


1. *Schaeffel, J.A., Ranson, W.F. and Swinson, W.F., "Acoustical-speckle Interferometry,"* EXPERIMENTAL MECHANICS, **20** *(4), 109-117 (April 1980).*
2. *Schaeffel, J.A. et al., Ibid.*
3. *Chu, T.C., "Digital Image Correlation Method in Experimental Mechanics," PhD Diss., Univ. of South Carolina (Dec. 1982).*
4. *Chu, T.C., Ranson, W.F. and Sutton, M.A., "Applications of Digital-Image-Correlation Techniques to Experimental Mechanics,"* EXPERIMENTAL MECHANICS, **25** *(3), 232-244 (Sept. 1985).*
5. *Peters, W.H., Ranson, W.F., Sutton, M.A. and Chu, T.C., "Applications of Digital Correlation Methods to Rigid Body Mechanics," Opt. Eng.,* **22** *(6), (Nov. 1983).*
6. *Peters, W.H. and Ranson, W.F., "Digital Imaging Techniques in Experimental Stress Analysis," Opt. Eng.,* **21** *(3), 427-432 (1982).*
7. *Chu, T.C., Peters, W.H., Ranson, W.F. and Sutton, M.A., "Digital Image Processing of Finite Deformations," Engineering Application of Optical Methods, Proc. 1983 SESA Spring Conf., 223-227 (May 1983).*
8. *Emmett, A., "Stereodigitize of Measurements of Auto Parts," Comp. Graphics World,* **8** *(10), 33-38 (Oct. 1985).*
9. *Klaus, B. and Horn, P., Robot Vision, The MIT Press, Cambridge, MA (1986).*
10. *Nevatia, R., Machine Perception, Prentice-Hall, Englewood Cliffs, NJ (1982).*
11. *Kahn-Jetter, Z.L., "Stereoscopic Principles Using Digital Image Correlation for Three-Dimensional Displacements," PhD Diss., Polytechnic Univ. (Aug. 1987).*
12. *Kahn-Jetter, Z.L., Ibid.*
13. *Wu, M.J., "Image Correlation and Image Display with Graphics and Pseudocolor Using Microcomputer," MS Thesis, Polytechnic Univ. of New York (May 1984).*